molecular pharmaceutics

Article

pubs.acs.org/molecularpharmaceutics

Low Intensity Ultrasound Mediated Liposomal Doxorubicin Delivery Using Polymer Microbubbles

Francois T. H. Yu, Xucai Chen, Jianjun Wang, Bin Qin, and Flordeliza S. Villanueva*

Center for Ultrasound Molecular Imaging and Therapeutics, University of Pittsburgh, Pittsburgh, Pennsylvania 15213, United States

Supporting Information

ABSTRACT: Cardiotoxicity is the major dose-limiting factor in the chemotherapeutic use of doxorubicin (Dox). A delivery vehicle that can be triggered to release its payload in the tumoral microvasculature but not in healthy tissue would help improve the therapeutic window of the drug. Delivery strategies combining liposomal encapsulated Dox (LDox), microbubbles (MBs), and ultrasound (US) have been shown to improve therapeutic efficacy of LDox, but much remains to be known about the mechanisms and the US conditions that maximize cytotoxicity using this approach. In this study, we compared different US pulses in terms of drug release and acute toxicity. Drug uptake and proliferation rates using low-intensity US were measured in squamous cell carcinoma cells exposed to LDox conjugated to or coinjected with polymer MBs. The aims of this study were: (1) to compare the effects of low- and high-pressure US on Dox release kinetics; (2) to evaluate whether conjugating the liposome to the MB surface (DoxLPX) is an important factor for drug release and cytotoxicity; and (3) to determine which US parameters most inhibit cell proliferation and whether this inhibition is mediated by drug release or the MB/US interaction with cells. Low-pressure US (170 kPa) at high duty cycle (stable cavitation) released up to ∼70% of the encapsulated Dox from the DoxLPX, thus improving Dox bioavailability and cellular uptake and leading to a significant reduction in cell proliferation at 48 h. Flow cytometry showed that US generating stable oscillations of DoxLPX significantly increased cellular Dox uptake at 4 h after US exposure compared to LDox. Drug uptake was correlated with cytotoxicity at 48 h. Our results demonstrate that Dox-containing liposomes conjugated to polymer MBs can be triggered to release ∼70% of their payload using noninertial US. Following release, Dox became bioavailable to the cells and induced significantly higher cytotoxicity compared to nonreleased encapsulated drug. Our findings show promise for targeted drug delivery using this theranostic delivery platform at low US intensities.

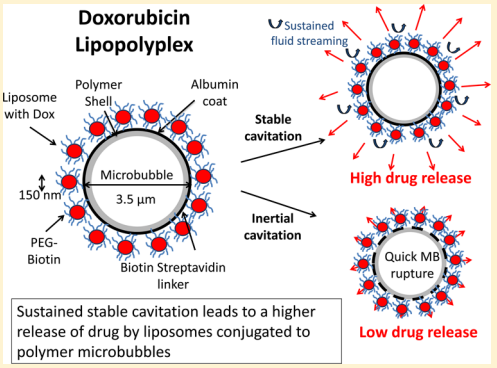

KEYWORDS: *ultrasound, microbubble, liposome, doxorubicin, cavitation, drug uptake*

1. INTRODUCTION

Doxorubicin (Dox) is part of the family of the anthracyclines, the class of antitumor drugs with the widest spectrum of activity in human cancers.[54] Dox is an amphiphilic 0.6 kDa molecule that can cross cellular membranes and accumulate in the nucleus. Dox antiproliferative cellular mechanisms include topoisomerase II inhibition, DNA intercalation, DNA cross-linking, generation of free radicals, and lipid peroxidation.[4,40,50] Similarly to other chemotherapeutic molecules, the therapeutic window of Dox is limited by systemic toxicity and more particularly by cardiotoxicity.[15]

Dox can be encapsulated for reduced systemic toxicity. Doxil (Johnson & Johnson, Titusville, NJ) is a liposomal formulation of Dox that is FDA-approved for treatment of ovarian cancer, advanced breast cancer, and Kaposi sarcoma.[43] When Dox is encapsulated in PEGylated liposomes composed of glycerophospholipids with 18 or more carbons, the resulting liposomes are very stable at physiological temperature, have a long plasma half-life (>48 h), and accumulate in the tumoral interstitial space through the enhanced permeability and retention effect.[3,23,28,38] However, despite improved biodistribution and cardiotoxicity profiles, Doxil has not been shown to have better efficacy in clinical trials compared to Dox.[33,40] This apparent contradiction is believed to be partly due to low drug bioavailability and poor penetration of the drug when it is in the liposomal form,[32,33,47,48] underscoring the fact that intratumoral liposome accumulation alone is insufficient to ensure drug bioavailability and the need to enhance drug release from the liposome itself. Liposomal doxorubicin therapy can cause serious side effects including mucositis and hand and foot syndrome, resulting from the accumulation of liposomes in the capillaries.

Microbubbles (MBs) are intravenously injectable gaseous spheres (1−5 μm diameter) stabilized by a shell (phospholipid, protein, or polymer) and used as blood tracers in ultrasound (US) imaging. When in an US field, MBs oscillate by expanding and compressing nonlinearly in response to the pressure wave,

Received: May 28, 2015
Revised: October 16, 2015
Accepted: November 15, 2015

DOI: 10.1021/acs.molpharmaceut.5b00421
Mol. Pharmaceutics XXXX, XXX, XXX−XXX

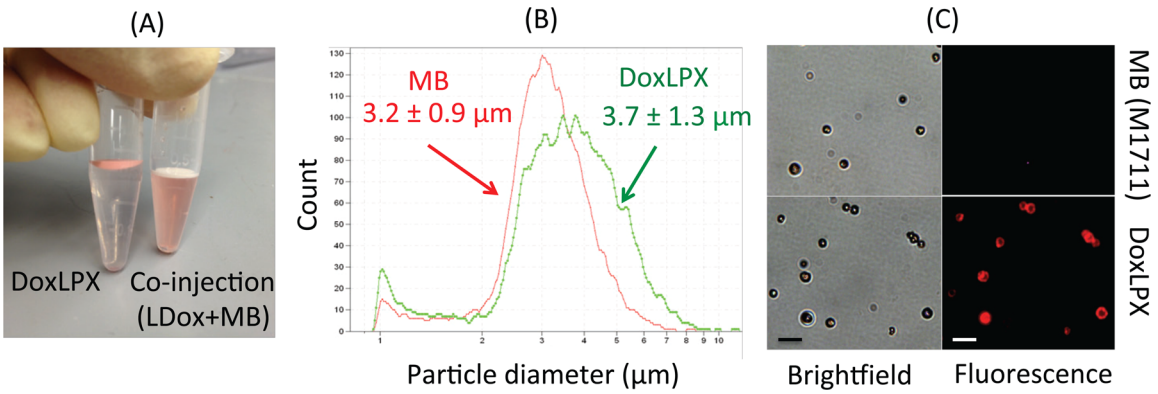

Figure 1. Characterization of DoxLPX. (A) After centrifugation, floating DoxLPX carry liposomes conjugated on the MB surface (DoxLPX), but liposomes coinjected with MB remained in the subnatant. (B) Size distribution (Coulter counter) of MBs before conjugation and DoxLPX after conjugation of doxorubicin liposomes. (C) Brightfield and fluorescence (470/590 nm) images of MB and DoxLPX. Scale bars 10 μm.

a phenomenon which is exploited for MB-specific US imaging. Interestingly, these oscillations can also cause *in vivo* bioeffects, including permeabilization of microvessels to colloidal particles,[44] opening of the blood brain barrier,[2,10,31,53] and enhancement of cellular permeability by sonoporation and endocytosis.[13,14,20,34,36,39] MB acoustic behaviors are classified into "stable" and "inertial" cavitation, which respectively occur at low and high incident acoustic pressures.[6,34,45,49] Stable cavitation (by generating acoustic streaming) and inertial cavitation (by creating a microjet upon MB inertial collapse) have been associated with therapeutic US applications in preclinical *in vivo* studies, notably for enhancing drug[5,18,25,52] and nucleic acid delivery.[7−9]

Several approaches have been described to incorporate Dox onto MB carriers to achieve US-targeted Dox delivery. Dox has been loaded in the MB lipid bilayer using electrostatic attraction and hydrophobic forces,[51] incorporated in the thick shell of polymer MBs,[11,16] or encapsulated into liposomes conjugated to lipid MBs.[12,17,24,35] The liposome/MB approach is attractive because it has the potential for high loading efficiency.[3] By using MBs, liposomes loaded with Dox, and US, studies have shown that *in vitro* cell proliferation decreased in an US-dependent manner for a variety of cell lines and US conditions,[12,17,24,35] raising promise for this delivery platform. The mechanisms thought to be implicated in the therapeutic cytotoxicity include: (1) MB/US induced liposomal drug release and cellular uptake;[17,35] (2) MB/US enhanced liposomal uptake and subsequent intracellular liposomal leakage;[17,35] (3) MB/US increased uptake of free Dox.[19] However, the relative contribution and importance of each hypothesized mechanism remains largely unknown. Furthermore, since mixtures of conjugated and coinjected liposomes were used in some of these studies (no washing of unattached liposomes after conjugation step),[17,24,35] it is difficult to determine if conjugation of the liposomes to the MB surface was critical to therapeutic efficacy.

Since free Dox can permeate cell membranes, Dox release is believed to be an important step for successful targeted delivery of the drug via carriers. Various US conditions have been reported to release Dox or other molecules from liposomes conjugated to lipid MB (lipoplexes) at high[17,30] and low US pressure.[35] However, the use of DPPC based liposomes,[17,35] which are known to be leaky at 37 °C,[28] introduces some uncertainty as to the mechanisms responsible for the reported toxicity.[1]

In this study, we investigated the performance of a new delivery platform utilizing liposomal Dox conjugated to polymer MBs in conjunction with US delivery parameters covering inertial and noninertial regimes. The use of a polymer MB confers several potential advantages. Polymer MBs are more stable and survive in the circulation for a longer time compared to lipid MBs.[21] Further, we have found that polymer MBs can load more drug than their lipid counterpart (see sections 3.1 and 4.1).

Accordingly, the aims of this study were: (1) to prepare a liposomal Dox formulation that is stable at physiological temperatures and can be loaded with high efficiency on polymer MB to form Dox lipopolyplexes (DoxLPX); (2) to compare the effects of long cycle, low-pressure US and high-pressure US of equal time-averaged intensity (<1.5 W/cm^2) on DoxLPX release kinetics and acute cytotoxicity; (3) to evaluate whether conjugating the liposome to the MB surface confers incremental Dox-induced cytotoxicity compared to simple coinjection of MB and Dox-encapsulated liposomes; and (4) to determine which US parameters caused the largest inhibition in cell proliferation and whether this is due to the drug delivery platform or merely a Dox-independent "side effect" of MB cavitation.

2. METHODS

2.1. Preparation of Dox-Containing Liposomes.

Biotinylated PEGylated liposomes were first prepared by thin film hydration and remote loaded with Dox using a pH gradient.[41] Briefly, 1,2-distearoyl-*sn*-glycero-3-phosphocholine (DSPC), cholesterol (Chol), and 1,2-distearoyl-*sn*-glycero-3-phosphoethanolamine-N-[biotinyl (polyethylene glycol)-2000] (DSPE-PEG-Biotin) were purchased (>99% purity, Avanti Polar Lipids Inc., Alabaster, AL) and mixed in 64:31:5 molar ratios. The chloroform was removed under a stream of argon gas, and the thin film was hydrated in a citrate buffer (pH 4.0, 0.3 mol/L). The liposomes were then gently sonicated briefly (Sonicator 75D,VWR, Radnor, PA) and frozen/thawed five times by successively immersing in liquid nitrogen and a 65 °C water bath. Next, the liposomes were extruded twice through polycarbonate membranes (400 and 200 nm pore size). The pH was adjusted to 7.0 with 0.5 mol/L of sodium carbonate before Dox (>98% purity, Cayman Chemical, Ann Arbor, MI) was remote loaded into the liposomes by adding a 10:1 (Lipid:Dox) molar ratio. The mixture was magnetically stirred (100 rpm) and incubated at 65 °C for 30 min. Free Dox was

DOI: 10.1021/acs.molpharmaceut.5b00421
Mol. Pharmaceutics XXXX, XXX, XXX−XXX

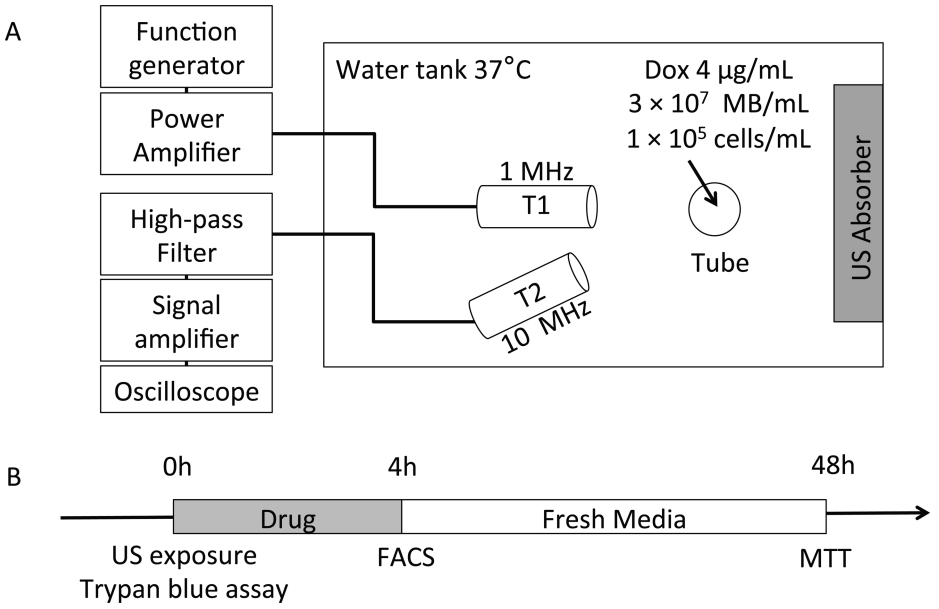

Figure 2. (A) Experimental setup for ultrasound exposure (T1, treatment transducer; T2, cavitation detection transducer) and (B) timeline for cell incubation and assay of acute viability after US exposure (Trypan Blue exclusion assay) and cell survival at 48 h (MTT assay).

then removed by passing the resulting mixture through a Sephadex column (GE Healthcare Biosciences, PD-10 column, Pittsburgh, PA). The average hydrodynamic diameter of the final liposomes was determined by dynamic light scattering (Malvern, Zetasizer, Worcestershire, UK). Liposomal Dox concentration was measured by fluorometry at excitation/emission wavelengths of 485/595 nm (Beckman Coulter, DTX-880 Multimode detector, Brea, CA) before and after the addition of 0.3% Triton X-100 to lyse the liposomes and dequenching the fluorescence of Dox.

2.2. Conjugation with Polymer MB. The polymer MBs (M1711, University of Pittsburgh, PA) used in this study were composed of an outer shell of cross-linked human albumin, an inner shell of polymer (poly-D,L-lactide), and a core of nitrogen gas. The surface of these MBs was coated with streptavidin for further attachment of cargos.[42] The liposomal DOX was conjugated to MBs via biotin−streptavidin interaction. Briefly, equal volumes of liposomes and MBs were mixed at room temperature for 1 h on a rotisserie shaker (Model # 400110, Barnstead Labquake, Thermo Scientific, Grand Island, NY). The excess liposomes in the subnatant were discarded after centrifugation (200 × *g* for 3 min), which yielded a final red colored floating DoxLPX preparation (Figure 1). The DoxLPX were counted and sized by a Coulter counter (Beckman Coulter, Multisizer 3, Brea, CA), and the amount of loaded Dox per bubble was assessed by fluorometry using 0.3% Triton X-100 detergent. Conjugation of the liposome to the MB surface was verified by fluorescence microscopy (IX81, with 60× objective, Olympus, Center Valley, PA) before and after LDox conjugation (Figure 1).

2.3. Cell Culture. *In vitro* studies were performed using murine squamous cell carcinoma cells (SCC7). SCC7 cells stocks were harvested from tumors induced in C3H mice and frozen, as described previously.[8,22] SCC7 cells used in this study were passaged less than 10 times before experiments.[7,8] Cells were cultured in media (RPMI-1640, Lonza, BioWhittaker, Basel, Switzerland) supplemented with 10% heat deactivated fetal bovine serum and 2% penicillin−streptomycin in a humidified incubator under 5% CO_2 at 37 °C and passaged every 2 days (passage number <10).

2.4. Assessment of Cytotoxicity. Cell viability was assessed at 10 min after US exposure using the trypan blue exclusion assay. Cells were incubated with 0.2% trypan blue for 1 min, and a minimum of 100 cells were counted on a hemocytometer (Bright Line, Hausser Scientific, Horsham PA) using an inverted microscope (Motic AE21, Scientific Instrument Company, Campbell, CA) in brightfield mode (Figure 2B). Cell viability was quantified as the number of live cells (absence of trypan blue staining) divided by the total number of cells. Experiments were repeated in three independent experiments.

Cell proliferation was assessed by MTT assay.[35] After US exposure, cells were placed in a 48-well plate (Falcon Multiwell, Becton Dickinson, San Jose, CA) and incubated at 37 °C in 5% CO_2. After 4 h, the supernatant was washed and replaced with 500 μL of fresh medium (Figure 2B). At 48 h, the media was removed, and the cells were incubated in 250 μL of 3-(4,5-dimethylthiazol-2-yl)-2,5-diphenyltetrazolium bromide (MTT, Sigma-Aldrich, Saint Louis, MO), diluted in phenol free Dulbecco's modified Eagle's medium (DMEM, Lonza, BioWhittaker, Basel, Switzerland) at a concentration of 0.2 mg/mL for 1.5 h at 37 °C and 5% CO_2, to allow the intracellular enzymatic reduction of MTT into purple formazan. The cells were then washed and incubated in 300 μL of dimethyl sulfoxide (DMSO, Sigma-Aldrich, Saint Louis, MO) and 25 μL of Sorenson's glycine buffer (0.1 M glycine, 0.1 M NaCl, pH = 10.5) for 10 min at room temperature. The optical density (OD) of the solubilized formazan was measured at 595 nm (DTX-880 Multimode Detector, Beckman Coulter, Brea, CA). Cell survival rate in sample *x* was calculated as a ratio of OD of the sample to that of the cells receiving no treatment using (adjusted for background of the untreated sample)

$$\text{Cell survival rate}_x = \frac{\text{OD}_x - \text{OD}_\text{T}}{\text{OD}_\text{NoTreatment} - \text{OD}_\text{T}} \quad (1)$$

DOI: 10.1021/acs.molpharmaceut.5b00421
Mol. Pharmaceutics XXXX, XXX, XXX−XXX

where OD_x, $OD_{NoTreatment}$, and OD_T are, respectively, the optical density of the measured sample, untreated sample, and of cells treated with 0.1% Triton X-100 (background signal from dead cells). Experiments were repeated in triplicate.

2.5. Comparison of Drug Effect between Dox and LDox. To compare the cytotoxic dose response of Dox and LDox (No US), 25 000 SCC7 cells were incubated with 0, 1.5, 3, 6, and 12 μg/mL of Dox or LDox in a 48-well plate. Medium (RPMI-1640, Lonza, BioWhittaker, Basel, Switzerland) supplemented with 10% heat deactivated fetal bovine serum and 2% penicillin−streptomycin was changed after 4 h, and cells were returned to the incubator. At 48 h, cell proliferation was measured using MTT assay as described earlier.

2.6. Experimental Setup and Ultrasound Delivery Protocol. The experimental setup is shown in Figure 2, panel A. Treatment US was provided by a 1 MHz flat single element transducer (Olympus, A303S, 0.5 in./flat, Waltham, MA), immersed in a degassed deionized water tank maintained at 37 °C, and excited with an arbitrary function generator (AFG3252, Tektronics, Beaverton, OR) and a power amplifier (250A250AM8, Amplifier Research, Souderton, PA).

The US pressure was calibrated using a bullet hydrophone (Model HGL-0200, Onda Corp, Sunnyvale, CA). High pressure treatment pulses (H), at fixed peak negative pressure of 1500 kPa, were five cycles (H1500−5), 643 cycles (H1500−643), and 2000 cycles (H1500−2k) long. Low pressure treatment pulses (L) of 50 000 cycle duration were at pressure of 170 kPa (L170−50k) and 300 kPa (L300−50k). The pulse repetition frequency was set at 10 Hz. Parameters were chosen to result in "high" and "low" pressure configurations with equivalent spatial peak temporal average intensity (I_{SPTA}) values. The pulse characteristics are summarized in Table 1. Attenuation was measured to be minimal (<5%), and therefore no attenuation correction was applied.

Table 1. US Pulses Used in This Study (All at 1 MHz)

pulse name	pressure (kPa)	no. cycles	duty cycle (%)	I_{SPTA} (W/cm^2)
H1500−5	1500	5	0.005%	0.0038
H1500−643	1500	643	0.64%	0.48
H1500−2k	1500	2000	2%	1.5
L170−50k	170	50000	50%	0.48
L300−50k	300	50000	50%	1.5

For each US study, a 500 μL volume of each experimental sample was held in a sterile polystyrene tube (5 mL round-bottom, BD Falcon, San Jose, CA), positioned at 41 mm from the treatment transducer surface, at a 30° angle from the vertical to minimize standing waves. The sample was gently agitated using a magnetic stir bar (100 rpm) continuously throughout the treatment procedure. MB and DoxLPX concentrations were fixed at 3×10^7 MB/mL, which corresponded to a Dox concentration of 4 μg/mL. An acoustic absorber was placed on the other side of the tube to reduce US reflection. A 10 MHz spherically focused single element transducer (V311, 0.5 in./F4, Olympus NDT, Waltham, MA) was confocally aligned on the sample volume at a 30° angle and was used in passive detection mode. The angle was chosen to be as small as possible to reduce the effects of MB attenuation on the cavitation data. The signal was high-pass filtered (HB5−2M-50−65B, 2 MHz high pass, TTE, Los Angeles, CA), amplified (5073PR, Olympus, Waltham, MA), and digitized using an oscilloscope (Waverunner 6051A, Teledyne Lecroy, Chestnut Ridge, NY). MBs could be observed to be pushed around in the sample tube by acoustic radiation force and were therefore periodically redistributed by gentle agitation every 15 s.

Time frequency analysis of the cavitation signal was performed offline with Matlab (Mathworks, Natick, MA) using a 50% overlapping sliding window of 10 μs duration on data sets digitized every 18 s for 3 min. The detected signals were averaged in the short time axis over the pulse duration (respectively, 50 ms, 2 ms, or 643 μs) to obtain the mean scattered power spectrum for each pulse at different time points during US treatment. Since MBs were disappearing during the treatment (due to the US), only representative spectra from the beginning of the treatment when MBs were present are reported. An example of MB and DoxLPX echogenicity is shown in Supplemental Figure S1.

2.7. Studies of US-Induced Dox Release. For drug release studies, US was delivered to 500 μL suspensions of LDox or DoxLPX for a total of 5 min using one of the pulse configurations shown in Table 1 and using the same experimental conditions as in section 2.6 but without cells. It is known that Dox fluorescence is quenched when entrapped in liposomes because it is in a crystalline form.[46] At the end of every minute of the 5 min US treatment, a 40 μL sample was taken from the tube, and free Dox was measured by fluorometry (DTX-880 Multimode detector, Beckman Coulter, Brea, CA) with excitation and emission wavelengths of 485 and 595 nm. Release at time t was calculated as

$$\text{release}\ (\%) = \frac{I_t - I_{t0}}{I_{\text{Triton}} - I_{t0}} \tag{2}$$

where I_{t0} is the fluorescence of the sample before US treatment, I_t is fluorescence at time t after US, and I_{Triton} is the fluorescence of the sample treated with 0.3% Triton X-100 (v/v), which lyses the liposomes. $(I_{\text{Triton}} - I_{t0})$ therefore corresponds to the 100% released drug fluorescence reference (see Supplemental Figure S2 for details).

2.8. Studies of US-Induced Dox Delivery. Effectiveness of Dox delivery under varying experimental conditions was evaluated using SCC7 cells. Cells (50 000) were suspended in 500 μL of media in capped sterile polystyrene tubes. DoxLPX or MB (at a final concentration of 3×10^7 MB/mL), or Dox or LDox (at an equivalent concentration of 4 μg Dox/mL), was added to the tube. US was delivered over 3 min during simultaneous cavitation detection using the pulse configurations shown in Table 1. After US exposure, 50 μL of sonicated samples was put aside for viability assay to evaluate US-related toxicity (trypan blue exclusion assay), 250 μL was plated for cell proliferation assays (MTT) to evaluate the success of Dox delivery, and 200 μL was reserved for drug uptake measurement with flow cytometry (Figure 2B).

Because cytotoxicity at 48 h is a composite measure of the desired Dox effect as well as any potential direct toxic effect of US, cytotoxicity related to the US alone was important to parcel out to evaluate the true efficacy of our platform for Dox delivery. We inferred that cell death immediately after the US procedure would be due to MB/US toxicity. Thus, to measure acute cell toxicity immediately after US exposure, cells (from the 50 μL sample collected as above) were spun down at 300 × g for 3 min, and trypan blue exclusion assay was performed.

DOI: 10.1021/acs.molpharmaceut.5b00421
Mol. Pharmaceutics XXXX, XXX, XXX−XXX

To measure cellular Dox uptake after US treatment, cells from the 200 μL sample collected as above were incubated for 4 h, and then Dox uptake was measured by flow cytometry (FACSCalibur, Becton Dickinson, San Jose, CA) (Figure 2B). Forward and side scattering intensities were used to gate Dox fluorescence signals originating from cells, which were measured in the FL-2 channel (excitation 488 nm/emission (585/42) nm). A minimum of 3000 events were used for cell uptake measurements. Experiments were repeated in triplicate.

2.9. Statistical Analysis. All data were expressed as mean ± standard deviation. Release and MTT assay results were analyzed using one-way ANOVA. Pairwise comparisons were obtained using Tukey's *post hoc* testing or Student *t* test (two-tailed). *P*-value <0.05 was considered statistically significant.

3. RESULTS

3.1. Liposome and DoxLPX Characterization. The LDox had a z-average size of 158.4 nm and polydispersity index of 0.218 as measured by dynamic light scattering. Conjugation of the LDox to the MBs slightly changed the average size of the MB from 3.2 ± 0.9 μm to 3.7 ± 1.3 μm (Figure 1, center), consistent with the successful loading of LDox on the MB surface. Loading was further confirmed by fluorescence microscopy (Figure 1, right). We experimentally measured, using a fluorescence dequenching assay using 0.3% Triton X-100, that a single MB could load 1.3×10^{-7} μg of Dox. The DoxLPX concentration used experimentally was fixed at 3×10^7 DoxLPX/mL, for a drug concentration of 4 μg/mL, which is in the range of concentration commonly used *in vitro*.[17,19] Assuming full coverage of the MB by liposomes, it can be calculated that each microbubble carried roughly 1600 liposomes. Finally, LDox stability in plasma at 37 °C was assessed by fluorometry and showed a gradual release of fluorescence, reaching 15% of total fluorescence after 60 min (see Supplemental Figure S3). Details on fluorometric Dox quantification accuracy and LDox loading efficiency are shown in Supplemental Figure S4.

3.2. Effect of Liposomal Encapsulation of Dox on Cytotoxicity. The comparative toxicities of LDox and Dox on SCC7 cells (without US) were assessed using an MTT assay at 48 h (Figure 3). At all studied doses, encapsulating Dox in liposomes reduced therapeutic efficacy (cytotoxicity) by about 40% ($p < 0.05$). LDox or Dox induced a monotonic dose response, which became different from control for doses ≥6.0 and ≥1.5 μg/mL, respectively. Interestingly, a dose of 12 μg of encapsulated Dox had a lower level of cytotoxic efficacy than 1.5 μg of Dox, which translates into an eight-fold decrease in Dox toxicity when encapsulated and is consistent with a previous report of reduced cytotoxicity for encapsulated Dox.[28,32,33]

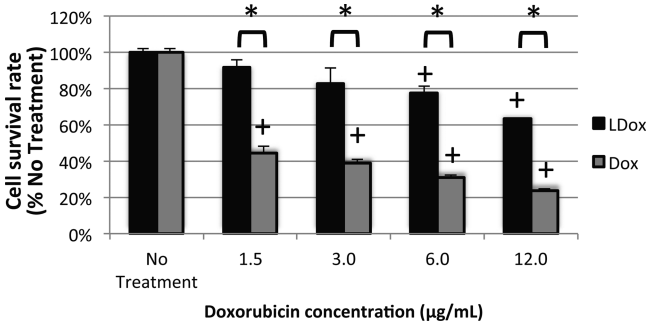

Figure 3. Survival rate of SCC7 cells exposed to free (Dox) and liposomal (LDox) doxorubicin as a function of doxorubicin concentration. Cells were exposed to the drug for 4 h, and the media was changed. Cell survival rate was measured by MTT at 48 h ($n = 3$). +, $p < 0.05$ versus no treatment. ∗, $p < 0.05$.

3.3. US Triggered Dox Release Kinetics: Dox Dequenching Assay. In Figure 4, panel A, DoxLPX+US release kinetics are shown over the 5 min treatment period for the acoustic pulses described in Table 1 (see raw fluorescence data in Supplemental Figure S2). DoxLPX+US release was computed using eq 2. The release kinetics could be divided into three subgroups: DoxLPX that were not exposed to US did not release Dox as a function of time ($p > 0.478$); DoxLPX+US exposed to H1500−2K, H1500−643, and H1500−5 released significantly more than DoxLPX(NoUS) ($p < 0.001$) at 5 min; DoxLPX+US with L170−50K and L300−50K pulses released the most drug ($p < 0.001$ vs all other pulses), respectively, 67 ± 5% and 49 ± 2% at 5 min. For the L170−50K pulse, release at 5 min was marginally different from release at 3 min ($p = 0.051$), whereas for the L300−50K, releases at 1 min and at later time points were not statistically different ($p > 0.123$). The effects of the L170−50K and H1500−2k pulses on the release kinetics of DoxLPX+US, LDox+MB+US and LDox+US are reported in Figure 4, panel B. LDox+US (without MB) did not release drug after 5 min with L170−50K and H1500−2k pulses ($p > 0.42$ vs DoxLPX[NoUS]). Coinjection of LDox and MB without conjugation respectively released only 11 ± 2% and 16 ± 5%, which was not different from DoxLPX(NoUS) ($p > 0.23$). Finally, in Figure 4, panel C, for the pulse at 170 kPa, changing the number of cycles (50 000, 5000, 500) but keeping the duty cycle the same (50%) by changing the pulse repetition frequency did not make a difference on Dox release ($p > 0.511$).

3.4. MB Cavitation Behavior and Acute Cellular Effects. Passive cavitation detection using a confocally aligned 10 MHz transducer was used to determine the MB oscillation behaviors associated with each pulse scheme shown in Table 1. Representative power spectra of the cavitation signal for L170−50K, L300−50K, H1500−643, and H1500−2k pulses are shown in Figure 5. L170−50K and L300−50K pulses scattered energy in fundamental and harmonic frequency bands. This is characteristic of low amplitude nonlinear MB oscillations and corresponds to the stable cavitation regime; no broadband signal was present. A dramatically different observation was found for the high-pressure pulses. For H1500−643 and H1500−2k, strong broadband signal (~20 dB above background) between the fundamental and harmonic peaks could be detected. The decrease in spectral power observed below 2 MHz was caused by the inline 2 MHz high-pass filter.

It is known that MB oscillations can induce acute cytotoxicity *in vitro*.[19,26] We therefore evaluated the cytotoxicity associated with pairs of L and H pulses with identical I_{SPTA} values (Figure 6) using a trypan exclusion assay after US exposure. The H pulses, which induced inertial cavitation (Figure 5), were acutely highly cytotoxic (>50% cytotoxicity, Figure 6). H1500−643 and H1500−2k pulses with DoxLPX+US caused a significant decrease in cell viability, which was respectively 38 ± 9% and 51 ± 5% immediately after US exposure (Figure 6). Since these H pulses did not induce drug release (Figure 4), we did not study these pulses further.

Interestingly, for the L pulses, the L170−50k had minimal acute toxicity, while the L300−50k significantly reduced acute cell viability, down to 55 ± 3% ($p < 0.001$) in the presence of

DOI: 10.1021/acs.molpharmaceut.5b00421
Mol. Pharmaceutics XXXX, XXX, XXX−XXX

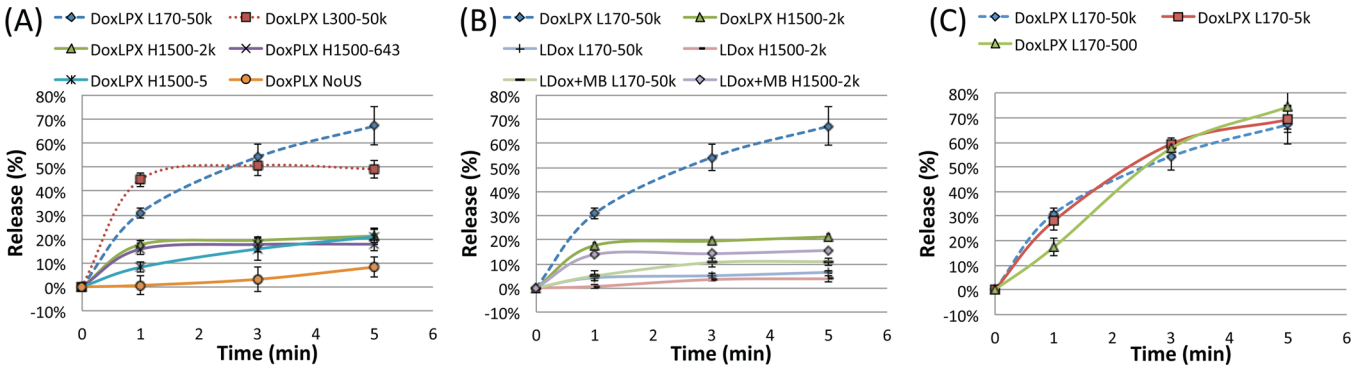

Figure 4. Kinetics of Dox fluorescence dequenching for: (A) DoxLPX exposed to different US pulses; (B) DoxLPX, nonconjugated liposomes and MB (LDox+MB), and liposomes (LDox) exposed to L170−50k and H1500−2k pulses; and (C) DoxLPX release kinetics for L pulses of 0.17 MPa with different pulse lengths but same duty cycle of 50% (n = 3).

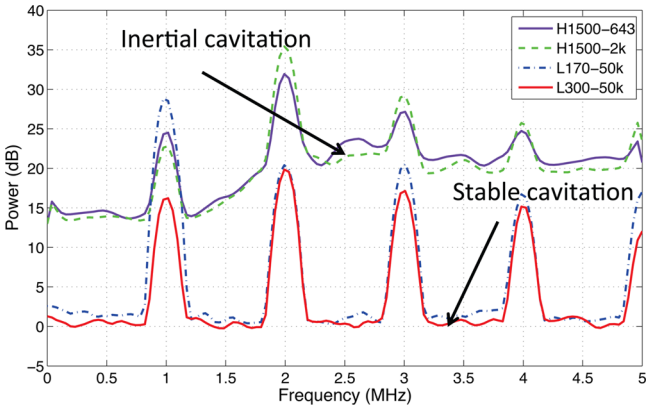

Figure 5. Representative cavitation spectra from MBs exposed to different US pulses.

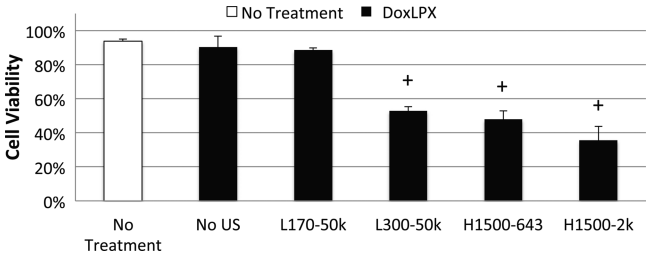

Figure 6. Acute cell viability (trypan exclusion assay) measured after 3 min of exposure of cells to DoxLPX using different ultrasound pulses (n = 3, + p < 0.05 vs no treatment).

MBs. Without MBs, L300−50k had no acute cytotoxicity (<5%, data not shown).

3.5. US-Induced Dox Delivery and Cellular Uptake. The L170−50k, which caused drug release without acute cytotoxicity (from US), was further studied to evaluate the efficacy of our drug delivery scheme as measured by cell survival at 48 h.

Acute viability with trypan exclusion assay was not affected by the L170−50k US pulse, irrespective of the presence of MB or drug (Figure 7). Cell survival at 48 h (to evaluate therapeutic cytotoxicity of the drug) is also shown in Figure 7. Survival rate for DoxLPX+US (49 ± 16%) and Dox (39 ± 3%) was significantly reduced versus no treatment (p < 0.05). Indeed, DoxLPX+US (L170−50k) had an equivalent therapeutic effect as Dox (p > 0.33). DoxLPX+US cell survival rate was also significantly lower (p < 0.05) than DoxLPX without US (84 ± 7%), LDox (84 ± 3%), LDox+US (89 ± 1%), and LDox+MB +US (coinjection, 85 ± 7%), indicating preferential cytotoxic activity of DoxLPX+US compared to all other encapsulated Dox-containing formulations. Importantly, empty lipopolyplexes (ELPX)+US caused neither acute nor 48 h cytotoxicity.

Drug uptake was quantified after 4 h of incubation using flow cytometry. Typical histograms of cellular fluorescence, measured in relative fluorescence units (RFU), are shown in Figure 8. Dox (313.6 ± 24.2) and DoxLPX+US (72.1 ± 12.4) groups had the highest drug uptake. DoxLPX+US uptake was significantly higher than no treatment (2.2 ± 0.4), LDox (14.8 ± 2.7), DoxLPX (19.5 ± 7.5), and LDox+MB+US (15.1 ± 2.3), but lower than Dox (p < 0.05). In summary, drug uptake was higher for DoxLPX+US compared to all encapsulated Dox formulations and equivalent or slightly lower than the sample

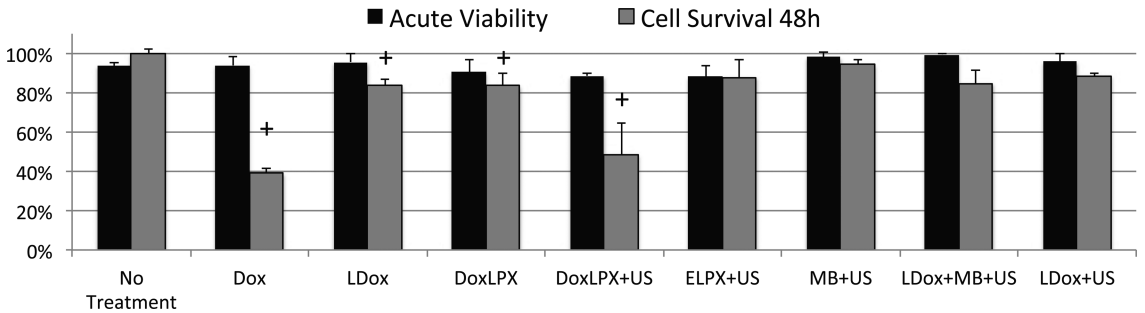

Figure 7. Cell viability (trypan exclusion assay) after US exposure (L170−50k pulse) and cell survival rate (MTT assay) at 48 h as a percentage of no treatment (n = 3, + p < 0.05 vs no treatment). ELPX = empty liposomes conjugated to MBs.

DOI: 10.1021/acs.molpharmaceut.5b00421
Mol. Pharmaceutics XXXX, XXX, XXX−XXX

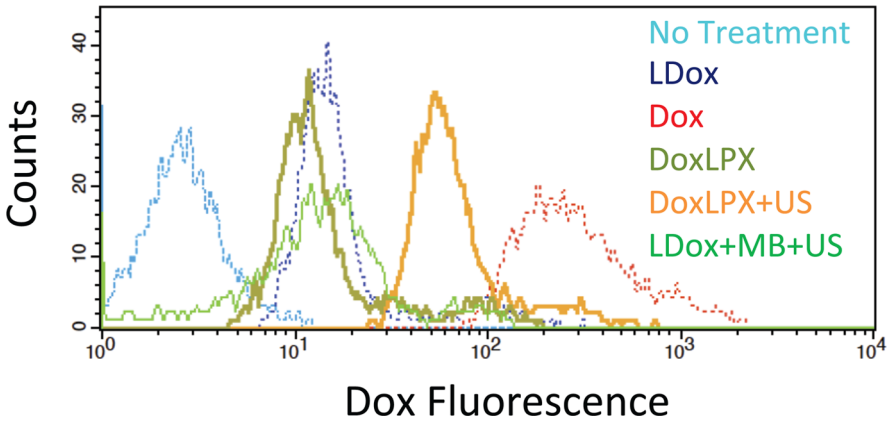

Figure 8. Histogram of cellular doxorubicin fluorescence after 4 h of incubation. Only DoxLPX+US and LDox+MB+US groups were exposed to US (L170−50k pulse) for 3 min.

incubated in Dox alone. Conjugating Dox to the MB surface was necessary for an increase in drug uptake, as the coinjection of LDox and MB in the presence of US resulted in less drug uptake than when these regimes were applied to DoxLPX.

3.6. Relationship between Drug Uptake and Cell Survival Rate. The relationship between cellular drug uptake and cell survival rate is represented in Figure 9. It can be seen that a logarithmic increase in uptake correlated with an increase in cell toxicity (toxicity = 1 − cell survival) for the L170−50k pulse (r^2 = 0.89, p < 0.001).

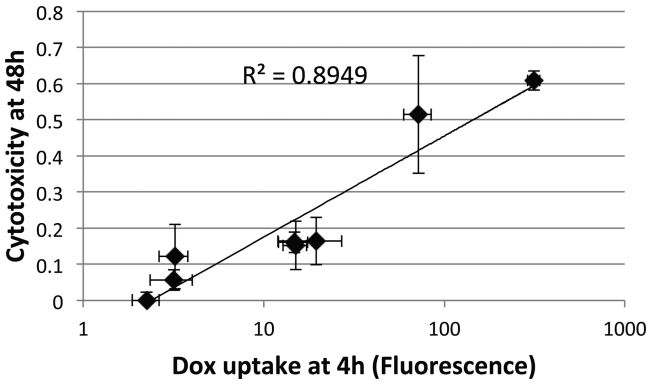

Figure 9. Doxorubicin uptake at 4 h (log scale) is directly correlated with cytotoxicity at 48 h.

4. DISCUSSION

This study investigated the mechanisms involved in US-mediated Dox delivery using liposomes and MBs. To do so, we fabricated nonleaky DSPC liposomes containing Dox and either conjugated or coinjected them with polymer MBs. We tested if Dox release from the liposomes was the major "active ingredient" for drug efficacy, under what US conditions maximal release occurred, and whether US delivered to MBs carrying Dox-encapsulated liposomes could increase cellular Dox concentration. Our main finding was that local delivery of Dox is improved by using non-inertial high duty cycle US and Dox-containing liposomes attached to polymer MBs. Because the efficacy of our platform is US-dependent, this approach is promising for US-triggered release and spatial (US image-guided) targeting of anthracyclines to tumoral tissues, while reducing toxicity to organs not receiving US, such as the heart, thus mitigating the cardiotoxicity, which is the major dose-limiting factor in anthracyclin-based chemotherapy. It is expected that this locally triggered release strategy will increase the ratio of tumoral/systemic exposure to bioavailable doxorubicin compared to systemic Dox and LDox.

4.1. Drug Encapsulation Stability and Loading on MB. Our data indicate that DSPC liposomes loaded with doxorubicin (LDox), which were stable at physiological temperature, could be conjugated to polymer MBs (Figure 1) to form an US triggered Dox delivery agent (DoxLPX). LDox maintained the drug encapsulated at 37 °C, as 4 h of incubation with the encapsulated drug failed to kill cells as compared to treatment with Dox (Figure 3). DoxLPX without US had the same stability as LDox (Figure 7), as reflected by low uptake at 4 h (Figure 8). This suggests that very low residual free Dox was present in our DoxLPX preparation, even after 4 h of incubation, which is consistent with low leakage from DSPC liposomes compared to DPPC liposomes.[28] We could load 1.3 × 10^{-7} μg of Dox per polymer MB. This is a four-fold improvement over reported loading capacities of lipid MB using the same biotin streptavidin chemistry[35] or electrostatic complexation,[51] and 26-times more than liposome−MB complexes formed using other chemistry.[17,24]

4.2. Important Parameters for Drug Release. We sought to quantify the effect of US regime and MB/liposome conjugation on Dox release from the liposome, as once Dox is released, it is permeable to cell membranes. When exposed to 3 min of low-pressure US (L170−50k and L300−50k pulses), which did not cause inertial cavitation (Figure 5), DoxLPX released over 50% of the loaded drug (Figure 4); however, for pulses with the same time-averaged intensity (H1500−643 and H1500−2k), which caused inertial cavitation (Figure 5), Dox release from DoxLPX was less than 20%. We also found that the high level of release was obtained only when LDox was conjugated with the MB and not when LDox was coinjected with MB (<20% release) nor when the LDox itself was exposed to US (<6% release). Temperature in the sample with the L170−50k and L300−50k pulses did not exceed 38 °C (Supplemental Figure S5) during US exposure, much lower than the DSPC liposome phase transition temperature (T_m = 51 °C), suggesting nonthermal release. Changing the pulse length while keeping the same duty cycle did not change the release kinetics (Figure 4C).

Since release occurred in the absence of broadband emission (Figure 5), our results suggest that drug release was mostly

DOI: 10.1021/acs.molpharmaceut.5b00421
Mol. Pharmaceutics XXXX, XXX, XXX−XXX

driven by sustained MB oscillations, radiation force, and agitation, which were persistently available throughout the US exposure with noninertial pulses. Conversely, high-pressure pulses also released some drug in a process involving inertial cavitation; however, these pulses rapidly destroyed the MB, which, as suggested by the data in Figure 4A showing an initial rapid rise then plateau in drug release for these pulsing schemes, was detrimental to the overall level of drug release. To our knowledge, this is the first quantification of a stable cavitation based release mechanism for liposomes conjugated on MBs.

The fact that the LDox required MB attachment for drug release supports the concept that very local fluid flow perturbations adjacent to a stably oscillating MB require the liposomes to be in close proximity to the MB to derive the "benefits" of these perturbations for drug release. Others have shown that 1 MHz US could trigger release from lipoplexes. Klibanov et al.[30] obtained ~30% release of calcein containing liposomes using 7 MPa pulses. The release levels we found with our H pulses (~20% release) are in line with these results. Escoffre et al. reported that 30 s of 600 kPa, 40% duty cycle pulses (likely inertial cavitation), could release up to >50% of the drug using DPPC (16 carbons) based liposomes.[17] By using the same liposome formulation (DPPC), cell proliferation data from Lentacker et al.[35] also suggest that some drug release can be obtained using a 15 s 170 kPa (likely noninertial cavitation), 40% duty cycle pulse. However, how much drug was actually released was not reported in that study. In a subsequent study by the same group,[24] US induced very limited release, although a different conjugation chemistry was used in that study. Direct comparisons between these studies and our study are difficult because different liposomes were used. Overall, such studies indicate that low pressures and high duty cycles are more efficient at releasing drug from liposomal Dox conjugated to MB.

4.3. Drug Uptake and Cytotoxicity. By using a lower pressure pulse (L170−50k), we obtained supporting evidence that release of Dox was the key mechanism involved in Dox cytotoxicity. With minimal acute MB/US toxicity (Figure 6), L170−50k caused a significant release of Dox (>50%) (Figure 4), which accumulated in the cells over the 4 h incubation (Figure 8) and caused a reduction in cell proliferation (Figure 7) that was correlated with the drug uptake at 4 h (Figure 9). With coinjection of LDox (unattached) and MBs, US did not produce release or uptake of LDox. LDox+MB+US cell survival rate was similar to LDox without MB. In these experiments, DoxLPX+US could not achieve higher therapeutic effect at 48 h compared to free Dox. Indeed, therapeutic effect was correlated with drug uptake at 4 h, which was lower for DoxLPX+US compared to Dox, consistent with an incomplete (~50%) release of Dox from DoxLPX+US. It is however expected that a local release of Dox guided by US would help reduce off-target Dox toxicity compared to a systemic Dox regimen.

4.4. MB/US Mediated Acute Toxicity. By using DoxLPX +US, we could obtain a higher cytotoxicity compared to Dox with the L300−50k pulse, which resulted in only 19.9 ± 4.7% of cell survival at 48 h (data not shown). However, by using this pulse, which was associated with drug release (Figure 4A), it appears that the US/MB acute toxicity (Figure 6) played a significant role in the final cytotoxicity. It is well-known that oscillations of MB near cells can cause permanent cell membrane damage leading to cell death.[26,27,29,37] In the context of drug delivery to tumors, acute cytotoxicity from MB/US may be therapeutically advantageous since the goal is to destroy tumors. However, it is important to distinguish this acute toxicity from the cellular drug delivery pathway to understand the mechanism leading to tumor growth inhibition. To this end, we measured acute toxicity immediately after US exposure. This is particularly important in conditions where released drug is present in the solution, as it has been shown that MB/US acute toxicity is accentuated in the presence of free Dox,[1] possibly by interfering with the cell membrane repair mechanisms.

As expected, acute toxicity generally increased with US intensity, as pulses with an I_{SPTA} of 1.5 W/cm^2 (L300−50k and H1500−2k) were more toxic than pulses with lower intensities.[26,37] However, since the nature of MB oscillations can vary significantly for a given I_{SPTA} based on US pressure and pulse length, ranging from stable oscillations at low pressure to violent inertial collapse at high pressure, we compared pulses with identical intensities but different pressures. Interestingly, L170−50k caused minimal acute toxicity, whereas H1500−643, a pulse with the same I_{SPTA} of 0.48 W/cm^2, was acutely toxic to cells. In our experiments, sustained stable cavitation caused less acute toxicity compared to inertial cavitation at the same I_{SPTA} level. Since MB/cell interactions depend on many parameters including MB type, charge and concentration, US parameters, and cell type,[19,20,26,27,29] our data suggest that that independent MB/US effects should be quantified systematically in therapeutic studies.

4.5. Study Limitations. While this study establishes important principles governing US-triggered drug release from liposomal formulations, studies were done *in vitro* in the absence of flow. The impact of Dox release kinetics on therapeutic efficacy is not fully measured in a static system, where the cells dwell with released drug, as compared to a system wherein drug loaded liposomes are transiting through the circulation. *In vivo* tumor models will be necessary to determine the ultimate therapeutic efficacy of this platform. Nonetheless, our findings establish important proof of concept and systematic optimization of this liposomal-MB US-triggered delivery platform. It is also important to note that some challenges remain to be addressed before clinical translation of the approach. Issues related to binding chemistry (replacing biotin−streptavidin with a covalent linking chemistry such as Maleimide−Thiol conjugates, for example), storage, and reconstitution (currently, polymer MBs, stored in a lyophilized form, are reconstituted in saline and conjugated to liposome on the day of the experiment) would ideally be performed in a single step prior to usage.

5. CONCLUSIONS

Our findings indicate that DoxLPX cytotoxicity using low-pressure US results from US mediated drug release from the liposomes, followed by diffusion of the drug into the cells, causing a reduction of cell survival rate. When Dox remained encapsulated (LDox, LDox+MB+US, and DoxLPX(NoUS)), Dox was not bioavailable to the cells and caused very low cytotoxicity at 48 h.

We have shown that for a given total acoustic energy, low pressure high duty cycle US (noninertial cavitation) results in more drug release than high pressure pulses (inertial cavitation). Release, uptake, and reduction of cell viability were reduced when LDox was coinjected with MBs. Therefore, our results suggest that liposomes should be attached to MBs for maximal cytotoxic effect. Also, we did not find evidence of

DOI: 10.1021/acs.molpharmaceut.5b00421
Mol. Pharmaceutics XXXX, XXX, XXX−XXX

an improved drug uptake with DoxLPX+US with low-intensity US compared to free Dox. This was mostly due to the capacity of free Dox to penetrate into the cells during the 4 h of incubation time, consistent with the established therapeutic efficacy of Dox.

By using polymer MBs, we were able to load significantly more drug than previously reported formulations using lipid MBs and liposomes. Polymer MBs are known to remain in circulation longer than lipid MBs, which should increase the *in vivo* targeting efficiency of the platform. Overall, this study raises promise for targeted Dox delivery using liposomes and MBs by using locally applied US energy. This versatile theranostic platform has high translational potential for any liposomal drugs that could benefit from local triggered intravascular delivery.

■ ASSOCIATED CONTENT

Supporting Information

The Supporting Information is available free of charge on the ACS Publications website at DOI: 10.1021/acs.molpharmaceut.5b00421.

MB and DoxLPX imaged in CPS 1.5 mode before and after high MI bursts; US induced fluorescence dequenching of DoxLPX exposed to L170−50k pulse at 1, 3, and 5 min; stability of LDox incubated in plasma at 37 °C; fluorescence of LDox with and without Triton with serial dilution in PBS showing linear fluorescence with dilution; Dox concentration based on fluorescence signal with Triton before and after passage through Sephadex column showing that most of the drug is encapsulated; total Dox concentration pre column assessed by fluorescence and by weight; maximal temperature reached during US treatment for listed US conditions (PDF)

■ AUTHOR INFORMATION

Corresponding Author

*E-mail: villanuevafs@upmc.edu. Phone: 412-647-5840. Fax: 412-647-4227.

Notes

The authors declare no competing financial interest.

■ ACKNOWLEDGMENTS

We would like to thank Regeant Panday for the technical assistance with the experiments. This work was partly funded by a postdoctoral fellowship grants (#27464) from "Fonds de recherche du Québec−Santé" (F.T.H.Y.) and by the Center for Ultrasound Molecular Imaging and Therapeutics, Heart and Vascular Institute, University of Pittsburgh. F.S.V. was supported in part by Grant Nos. 1R01EB016516-01A1 and R21 CA167373-01 from the National Institutes of Health.

■ ABBREVIATIONS

Ctrl, no treatment control; Dox, Doxorubicin; DoxLPX, Dox lipopolyplex = LDox on MB; EPLX, empty lipopolyplex; H pulse, high pressure US pulse; LDox, Doxorubicin encapsulated in liposomes; LPX, lipopolyplex = polymer MB carrying liposomes on its surface; L pulse, low pressure US pulse; MB, microbubble; SCC, squamous cell carcinoma; US, ultrasound

■ REFERENCES

(1) Afadzi, M.; Strand, S. P.; Nilssen, E. A.; Masoy, S. E.; Johansen, T. F.; Hansen, R.; Angelsen, B. A.; de L Davies, C. Mechanisms of the ultrasound-mediated intracellular delivery of liposomes and dextrans. *IEEE Trans Ultrason Ferroelectr Freq Control* **2013**, *60* (1), 21−33.

(2) Alkins, R.; Burgess, A.; Ganguly, M.; Francia, G.; Kerbel, R.; Wels, W. S.; Hynynen, K. Focused ultrasound delivers targeted immune cells to metastatic brain tumors. *Cancer Res.* **2013**, *73* (6), 1892−9.

(3) Barenholz, Y. Doxil (R) - The first FDA-approved nano-drug: Lessons learned. *J. Controlled Release* **2012**, *160* (2), 117−134.

(4) Burden, D. A.; Osheroff, N. Mechanism of action of eukaryotic topoisomerase II and drugs targeted to the enzyme. *Biochim. Biophys. Acta, Gene Struct. Expression* **1998**, *1400* (1−3), 139−54.

(5) Burke, C. W.; Alexander, E. t.; Timbie, K.; Kilbanov, A. L.; Price, R. J. Ultrasound-activated Agents Comprised of 5FU-bearing Nanoparticles Bonded to Microbubbles Inhibit Solid Tumor Growth and Improve Survival. *Mol. Ther.* **2014**, *22*, 321.

(6) Burke, C. W.; Price, R. J. Contrast ultrasound targeted treatment of gliomas in mice via drug-bearing nanoparticle delivery and microvascular ablation. *J. Visualized Exp.* **2010**, *15* (46), 2145.

(7) Carson, A. R.; McTiernan, C. F.; Lavery, L.; Grata, M.; Leng, X.; Wang, J.; Chen, X.; Villanueva, F. S. Ultrasound-Targeted Microbubble Destruction to Deliver siRNA Cancer Therapy. *Cancer Res.* **2012**, *72* (23), 6191−6199.

(8) Carson, A. R.; McTiernan, C. F.; Lavery, L.; Hodnick, A.; Grata, M.; Leng, X.; Wang, J.; Chen, X.; Modzelewski, R. A.; Villanueva, F. S. Gene therapy of carcinoma using ultrasound-targeted microbubble destruction. *Ultrasound Med. Biol.* **2011**, *37* (3), 393−402.

(9) Chen, S.; Shimoda, M.; Wang, M. Y.; Ding, J.; Noguchi, H.; Matsumoto, S.; Grayburn, P. A. Regeneration of pancreatic islets in vivo by ultrasound-targeted gene therapy. *Gene Ther.* **2010**, *17* (11), 1411−20.

(10) Choi, J. J.; Selert, K.; Vlachos, F.; Wong, A.; Konofagou, E. E. Noninvasive and localized neuronal delivery using short ultrasonic pulses and microbubbles. *Proc. Natl. Acad. Sci. U. S. A.* **2011**, *108* (40), 16539−44.

(11) Cochran, M. C.; Eisenbrey, J.; Ouma, R. O.; Soulen, M.; Wheatley, M. A. Doxorubicin and paclitaxel loaded microbubbles for ultrasound triggered drug delivery. *Int. J. Pharm.* **2011**, *414* (1−2), 161−70.

(12) Deng, Z.; Yan, F.; Jin, Q.; Li, F.; Wu, J.; Liu, X.; Zheng, H. Reversal of multidrug resistance phenotype in human breast cancer cells using doxorubicin-liposome-microbubble complexes assisted by ultrasound. *J. Controlled Release* **2014**, *174*, 109−16.

(13) Derieppe, M.; Rojek, K.; Escoffre, J. M.; de Senneville, B. D.; Moonen, C.; Bos, C. Recruitment of endocytosis in sonopermeabilization-mediated drug delivery: a real-time study. *Phys. Biol.* **2015**, *12* (4), 046010.

(14) Derieppe, M.; Yudina, A.; Lepetit-Coiffe, M.; de Senneville, B. D.; Bos, C.; Moonen, C. Real-time assessment of ultrasound-mediated drug delivery using fibered confocal fluorescence microscopy. *Mol. Imaging Biol.* **2013**, *15* (1), 3−11.

(15) Drummond, D. C.; Meyer, O.; Hong, K.; Kirpotin, D. B.; Papahadjopoulos, D. Optimizing liposomes for delivery of chemotherapeutic agents to solid tumors. *Pharmacol. Rev.* **1999**, *51* (4), 691−743.

(16) Eisenbrey, J. R.; Burstein, O. M.; Kambhampati, R.; Forsberg, F.; Liu, J. B.; Wheatley, M. A. Development and optimization of a doxorubicin loaded poly(lactic acid) contrast agent for ultrasound directed drug delivery. *J. Controlled Release* **2010**, *143* (1), 38−44.

(17) Escoffre, J. M.; Mannaris, C.; Geers, B.; Novell, A.; Lentacker, I.; Averkiou, M.; Bouakaz, A. Doxorubicin liposome-loaded microbubbles for contrast imaging and ultrasound-triggered drug delivery. *IEEE Trans Ultrason Ferroelectr Freq Control* **2013**, *60* (1), 78−87.

(18) Escoffre, J. M.; Novell, A.; Serriere, S.; Lecomte, T.; Bouakaz, A. Irinotecan delivery by microbubble-assisted ultrasound: in vitro validation and a pilot preclinical study. *Mol. Pharmaceutics* **2013**, *10* (7), 2667−75.

DOI: 10.1021/acs.molpharmaceut.5b00421
Mol. Pharmaceutics XXXX, XXX, XXX−XXX

(19) Escoffre, J. M.; Piron, J.; Novell, A.; Bouakaz, A. Doxorubicin delivery into tumor cells with ultrasound and microbubbles. *Mol. Pharmaceutics* **2011**, *8* (3), 799−806.
(20) Fan, Z.; Chen, D.; Deng, C. X. Improving ultrasound gene transfection efficiency by controlling ultrasound excitation of microbubbles. *J. Controlled Release* **2013**, *170* (3), 401−413.
(21) Ferrara, K.; Pollard, R.; Borden, M. Ultrasound microbubble contrast agents: fundamentals and application to gene and drug delivery. *Annu. Rev. Biomed. Eng.* **2007**, *9*, 415−47.
(22) Fu, K. K.; Rayner, P. A.; Lamx, K. N. Modification of the effects of continuous low dose rate irradiation by concurrent chemotherapy infusion. *Int. J. Radiat. Oncol., Biol., Phys.* **1984**, *10* (8), 1473−8.
(23) Gabizon, A.; Goren, D.; Cohen, R.; Barenholz, Y. Development of liposomal anthracyclines: from basics to clinical applications. *J. Controlled Release* **1998**, *53* (1−3), 275−9.
(24) Geers, B.; Lentacker, I.; Sanders, N. N.; Demeester, J.; Meairs, S.; De Smedt, S. C. Self-assembled liposome-loaded microbubbles: The missing link for safe and efficient ultrasound triggered drug-delivery. *J. Controlled Release* **2011**, *152* (2), 249−56.
(25) Goertz, D. E.; Todorova, M.; Mortazavi, O.; Agache, V.; Chen, B.; Karshafian, R.; Hynynen, K. Antitumor effects of combining docetaxel (taxotere) with the antivascular action of ultrasound stimulated microbubbles. *PLoS One* **2012**, *7* (12), e52307.
(26) Guzman, H. R.; Nguyen, D. X.; Khan, S.; Prausnitz, M. R. Ultrasound-mediated disruption of cell membranes. I. Quantification of molecular uptake and cell viability. *J. Acoust. Soc. Am.* **2001**, *110* (1), 588−96.
(27) Guzman, H. R.; Nguyen, D. X.; Khan, S.; Prausnitz, M. R. Ultrasound-mediated disruption of cell membranes. II. Heterogeneous effects on cells. *J. Acoust. Soc. Am.* **2001**, *110* (1), 597−606.
(28) Horowitz, A. T.; Barenholz, Y.; Gabizon, A. A. In vitro cytotoxicity of liposome-encapsulated doxorubicin: dependence on liposome composition and drug release. *Biochim. Biophys. Acta, Biomembr.* **1992**, *1109* (2), 203−9.
(29) Karshafian, R.; Bevan, P. D.; Williams, R.; Samac, S.; Burns, P. N. Sonoporation by ultrasound-activated microbubble contrast agents: effect of acoustic exposure parameters on cell membrane permeability and cell viability. *Ultrasound Med. Biol.* **2009**, *35* (5), 847−60.
(30) Klibanov, A. L.; Shevchenko, T. I.; Raju, B. I.; Seip, R.; Chin, C. T. Ultrasound-triggered release of materials entrapped in microbubble-liposome constructs: a tool for targeted drug delivery. *J. Controlled Release* **2010**, *148* (1), 13−7.
(31) Konofagou, E. E. Optimization of the ultrasound-induced blood-brain barrier opening. *Theranostics* **2012**, *2* (12), 1223−37.
(32) Laginha, K. M.; Verwoert, S.; Charrois, G. J.; Allen, T. M. Determination of doxorubicin levels in whole tumor and tumor nuclei in murine breast cancer tumors. *Clin. Cancer Res.* **2005**, *11* (19), 6944−6949.
(33) Lao, J.; Madani, J.; Puertolas, T.; Alvarez, M.; Hernandez, A.; Pazo-Cid, R.; Artal, A.; Anton Torres, A. Liposomal Doxorubicin in the treatment of breast cancer patients: a review. *J. Drug Delivery* **2013**, *2013*, 1−12.
(34) Lentacker, I.; De Cock, I.; Deckers, R.; De Smedt, S. C.; Moonen, C. T. Understanding ultrasound induced sonoporation: Definitions and underlying mechanisms. *Adv. Drug Delivery Rev.* **2014**, *72*, 49.
(35) Lentacker, I.; Geers, B.; Demeester, J.; De Smedt, S. C.; Sanders, N. N. Design and evaluation of doxorubicin-containing microbubbles for ultrasound-triggered doxorubicin delivery: cytotoxicity and mechanisms involved. *Mol. Ther.* **2010**, *18* (1), 101−8.
(36) Lepetit-Coiffe, M.; Yudina, A.; Poujol, C.; de Oliveira, P. L.; Couillaud, F.; Moonen, C. T. Quantitative evaluation of ultrasound-mediated cellular uptake of a fluorescent model drug. *Mol. Imaging Biol.* **2013**, *15* (5), 523−33.
(37) Liu, Y.; Yan, J.; Prausnitz, M. R. Can ultrasound enable efficient intracellular uptake of molecules? A retrospective literature review and analysis. *Ultrasound Med. Biol.* **2012**, *38* (5), 876−88.
(38) Manzoor, A. A.; Lindner, L. H.; Landon, C. D.; Park, J. Y.; Simnick, A. J.; Dreher, M. R.; Das, S.; Hanna, G.; Park, W.; Chilkoti, A.; Koning, G. A.; ten Hagen, T. L.; Needham, D.; Dewhirst, M. W. Overcoming limitations in nanoparticle drug delivery: triggered, intravascular release to improve drug penetration into tumors. *Cancer Res.* **2012**, *72* (21), 5566−75.
(39) Meijering, B. D.; Juffermans, L. J.; van Wamel, A.; Henning, R. H.; Zuhorn, I. S.; Emmer, M.; Versteilen, A. M.; Paulus, W. J.; van Gilst, W. H.; Kooiman, K.; de Jong, N.; Musters, R. J.; Deelman, L. E.; Kamp, O. Ultrasound and microbubble-targeted delivery of macromolecules is regulated by induction of endocytosis and pore formation. *Circ. Res.* **2009**, *104* (5), 679−687.
(40) Minotti, G.; Menna, P.; Salvatorelli, E.; Cairo, G.; Gianni, L. Anthracyclines: molecular advances and pharmacologic developments in antitumor activity and cardiotoxicity. *Pharmacol. Rev.* **2004**, *56* (2), 185−229.
(41) Niu, G.; Cogburn, B.; Hughes, J. Preparation and characterization of doxorubicin liposomes. *Methods Mol. Biol.* **2010**, *624*, 211−9.
(42) Ottoboni, S.; Short, R. E.; Kerby, M. B.; Tickner, E. G.; Steadman, E.; Ottoboni, T. B. Characterization of the in vitro adherence behavior of ultrasound responsive double-shelled microspheres targeted to cellular adhesion molecules. *Contrast Media Mol. Imaging* **2006**, *1* (6), 279−90.
(43) Park, J. W. Liposome-based drug delivery in breast cancer treatment. *Breast Cancer Res.* **2002**, *4* (3), 95−99.
(44) Price, R. J.; Skyba, D. M.; Kaul, S.; Skalak, T. C. Delivery of colloidal particles and red blood cells to tissue through microvessel ruptures created by targeted microbubble destruction with ultrasound. *Circulation* **1998**, *98* (13), 1264−7.
(45) Qin, S.; Caskey, C. F.; Ferrara, K. W. Ultrasound contrast microbubbles in imaging and therapy: physical principles and engineering. *Phys. Med. Biol.* **2009**, *54* (6), R27−57.
(46) Schroeder, A.; Kost, J.; Barenholz, Y. Ultrasound, liposomes, and drug delivery: principles for using ultrasound to control the release of drugs from liposomes. *Chem. Phys. Lipids* **2009**, *162* (1−2), 1−16.
(47) Song, G.; Wu, H.; Yoshino, K.; Zamboni, W. C. Factors affecting the pharmacokinetics and pharmacodynamics of liposomal drugs. *J. Liposome Res.* **2012**, *22* (3), 177−92.
(48) Sugahara, K. N.; Teesalu, T.; Karmali, P. P.; Kotamraju, V. R.; Agemy, L.; Greenwald, D. R.; Ruoslahti, E. Coadministration of a tumor-penetrating peptide enhances the efficacy of cancer drugs. *Science* **2010**, *328* (5981), 1031−5.
(49) Sutton, J. T.; Haworth, K. J.; Pyne-Geithman, G.; Holland, C. K. Ultrasound-mediated drug delivery for cardiovascular disease. *Expert Opin. Drug Delivery* **2013**, *10* (5), 573−92.
(50) Swift, L. P.; Rephaeli, A.; Nudelman, A.; Phillips, D. R.; Cutts, S. M. Doxorubicin-DNA adducts induce a non-topoisomerase II-mediated form of cell death. *Cancer Res.* **2006**, *66* (9), 4863−71.
(51) Tinkov, S.; Winter, G.; Coester, C.; Bekeredjian, R. New doxorubicin-loaded phospholipid microbubbles for targeted tumor therapy: Part I–Formulation development and in-vitro characterization. *J. Controlled Release* **2010**, *143* (1), 143−50.
(52) Todorova, M.; Agache, V.; Mortazavi, O.; Chen, B.; Karshafian, R.; Hynynen, K.; Man, S.; Kerbel, R. S.; Goertz, D. E. Antitumor effects of combining metronomic chemotherapy with the antivascular action of ultrasound stimulated microbubbles. *Int. J. Cancer* **2013**, *132* (12), 2956−66.
(53) Tung, Y. S.; Marquet, F.; Teichert, T.; Ferrera, V.; Konofagou, E. E. Feasibility of noninvasive cavitation-guided blood-brain barrier opening using focused ultrasound and microbubbles in nonhuman primates. *Appl. Phys. Lett.* **2011**, *98* (16), 163704.
(54) Weiss, R. B. The anthracyclines: will we ever find a better doxorubicin? *Semin. Oncos.* **1992**, *19* (6), 670−86.

DOI: 10.1021/acs.molpharmaceut.5b00421
Mol. Pharmaceutics XXXX, XXX, XXX−XXX